이학석사 학위논문

Magnetic resonance imaging texture changes of medial pulvinar in dementia with Lewy bodies patients

루이소체 치매 환자에서 내측 베개핵의 자기 공명 영상 텍스처 변화

2020년 2월

서울대학교 대학원

뇌인지과학과 뇌인지과학전공

탁 가 영

Magnetic resonance imaging texture changes of medial pulvinar in dementia with Lewy bodies patients

지도 교수 김 기 웅

이 논문을 이학석사 학위논문으로 제출함
2019년 12월

서울대학교 대학원
뇌인지과학과 뇌인지과학전공
탁 가 영

탁가영의 이학석사 학위논문을 인준함
2019년 12월

위 원 장 권 준 수 (인)

부위원장 김 기 웅 (인)

위 원 김 의 태 (인)

Abstract

Magnetic resonance imaging texture changes of medial pulvinar in dementia with Lewy bodies patients

Kayeong Tak

Department of Brain and Cognitive Sciences

The Graduate School

Seoul National University

Introduction: Executive dysfunction is common in dementia with Lewy bodies (DLB). The pulvinar nucleus plays a role in executive control, and synchronizes with cortical regions in the salience network that are vulnerable to Lewy pathology.

Objective: We investigated the pulvinar subregions in patients with mild DLB and their associations with executive function.

Methods: The sample consisted of 38 DLB patients and 38 age- and sex-matched normal controls. We evaluated cognitive function using the Consortium to Establish a Registry for Alzheimer's Disease Assessment Packet. We obtained four pulvinar nuclei using preprocessed T1-weighted magnetic resonance images. We compared volumes and textures of the DLB patients and the normal controls for each nucleus. We used a linear regression to determine the association of textures and

neuropsychological test scores.

Results: The DLB patients showed comparable volumes to the normal controls in all pulvinar nuclei. However, the DLB patients showed different texture of the left medial pulvinar (PuM) from the normal controls. The entropy, contrast and cluster shade were lower but autocorrelation of left PuM was higher in the DLB patients compared to the normal controls. These texture features of the left PuM were associated with the set-shifting performance measured by the trail making tests.

Conclusions: In DLB, the left PuM may be altered from early stage, which may contribute to the development of executive dysfunction.

Keywords: Dementia with Lewy bodies; Pulvinar nuclei; Texture analysis; Gray-Level Co-occurrence Matrix (GLCM)

Student Number: 2017-25754

Table of Contents

1. Introduction

1.1. Study Background

Dementia with Lewy bodies (DLB) is the second most common neurodegenerative dementia after Alzheimer's disease (AD). Lewy body pathology results from alpha-synuclein aggregation in nerve cells of the neocortical, limbic, and brainstem regions (McKeith et al., 2005; Spillantini et al., 1997). DLB is clinically characterized by progressive cognitive decline in addition to core clinical features, such as fluctuating cognition, recurrent visual hallucinations, and parkinsonism (McKeith et al., 2005). In the mild stage, DLB patients had more rapid cognitive decline than AD patients (Rongve et al., 2016). The cognitive impairment is more likely associated with nonamnestic domains, such as attention and executive function (Ferman et al., 2013; Petrova et al., 2016). Executive dysfunction may be caused by atrophy of the insular and anterior cingulate cortices in the early stage of DLB (Blanc et al., 2016; Blanc et al., 2015). The early vulnerable regions compose the salience network (SN) that initiates cognitive control as it modulates the switch between default mode network (DMN) and central executive network (CEN) (Sridharan, Levitin, & Menon, 2008). Since connectivity within the SN decreased in DLB patients (Lowther, O'Brien, Firbank, & Blamire, 2014), executive function can be declined.

The pulvinar of the thalamus is divided into 4 nuclei: anterior pulvinar (PuA), medial pulvinar (PuM), lateral pulvinar (PuL) and inferior pulvinar (PuI) (Olszewski, 1952). Although the pulvinar was commonly referred to as the visual pulvinar (Bridge, Leopold, & Bourne, 2016), the structure also contributed to executive function (Ouhaz,

Fleming, & Mitchell, 2018). In particular, the PuM has widespread connections with the prefrontal cortex and association areas, including the vulnerable regions in SN (Homman-Ludiye & Bourne, 2019; Romanski, Giguere, Bates, & Goldman-Rakic, 1997; Rosenberg, Mauguiere, Catenoix, Faillenot, & Magnin, 2008). Previous studies using functional magnetic resonance imaging (fMRI) found that the PuM mirrors SN connectivity in other diseases (Fredericks et al., 2019; S. E. Lee et al., 2014). Moreover, in recent postmortem studies on DLB patients, Lewy body pathology was present throughout the pulvinar but was most severe in the medial pulvinar (Erskine et al., 2017). However, the volume of anteromedial pulvinar was comparable between DLB patients and the normal controls (Erskine et al., 2017).

1.2. Purpose of Research

Until now, there were no structural or functional neuroimaging studies on the pulvinar nucleus of DLB patients in vivo. Since the volume of pulvinar did not reflect the Lewy pathology of medial pulvinar in a postmortem study, the volumetric study on brain magnetic resonance imaging (MRI) may not detect the neuronal degeneration of pulvinar in DLB patients. In contrast to the volumetric measures, the texture measures can identify changes at the neuronal level on brain MRI, because gray matter neuronal density was inversely associated with the T1 relaxation time (Goubran et al., 2015). Neuronal losses decrease macromolecules and increase extracellular water content, and thus, increase the T1 relaxation time and reduce the signal intensity on MRI. Neuronal destruction, as well as neuronal loss, also decrease the signal intensity on MRI (Gowland & Stevenson, 2003). To investigate the possible changes of the PuM and their association with executive dysfunction in DLB, we examined the changes in the volume

and texture of the pulvinar nuclei, and their association with neuropsychological test performance.

2. Methods

2.1. Subjects

We recruited 38 DLB patients from the dementia clinic of Seoul National University Bundang Hospital (SNUBH). We enrolled 38 age- and sex-matched cognitively normal controls (NC) from the participants of the Korean Longitudinal Study on Cognitive Aging and Dementia (KLOSCAD), which is a nationwide population-based prospective cohort study on cognitive aging and dementia launched in 2009 (Han et al., 2018). The characteristics of the subjects are summarized in Table 1. All patients (or their guardians) and control subjects were fully informed about the study, and written consent was obtained from them. The study was approved by the Institutional Review Board of the Seoul National University Bundang Hospital (SNUBH), Republic of Korea.

2.2. Assessments

Geriatric neuropsychiatrists performed a standardized diagnostic interview, physical and neurological examinations, and laboratory tests for all participants using the Korean version of the Mini International Neuropsychiatric Interview (MINI) (Yoo et al., 2006) and the Consortium to Establish a Registry for Alzheimer's Disease Assessment Packet (CERAD-K) Clinical Assessment Battery (J. H. Lee et al., 2002). Trained research neuropsychologists or nurses evaluated global cognitive function using the Mini-Mental Status Examination (MMSE) to ascertain the presence of cognitive impairment. We diagnosed DLB based on the consensus guidelines proposed by McKeith et al. (McKeith

et al., 2005), and determined the global severity of dementia by the Clinical Dementia Rating (CDR) (Morris, 1993). We performed the digit span (forward and backward) by scoring 1 or 0 (pass or fail) to repeat the sequence, and the Trail Making Test (TMT-A and TMT-B) by measuring time to connect distributed numbers, or numbers and letters alternately in ascending order (J. H. Lee et al., 2002; Wechsler, 1987).

2.3. Neuroimaging analysis

All subjects underwent three-dimensional structural T1-weighted spoiled gradient echo MRI scanning on a 3.0 Tesla GE SIGNA scanner (GE Healthcare, Milwaukee, USA) within one and a half years from the clinical assessments. The MRI images were obtained based on the following parameters: voxel size of 1.0 x 0.5 x 0.5 mm^3, 1.0 mm sagittal slices thickness with no inter-slice gap, echo time (TE) of 3.68 ms, repetition time (TR) of 25.0 ms, number of excitations (NEX) of 1, flip angle of 90°, field of view (FOV) of 240 x 240 mm, and 175 x 240 x 240 matrix in the x-, y-, and z-dimensions. To exclude subjects with the risk of concomitant vascular pathology, T2-weighted FLAIR MRI was obtained with the 3.0 Tesla scanner system (GE Healthcare, Milwaukee, USA) using the following protocols: voxel size of 0.5 x 0.5 x 3.0 mm^3, 3.0 mm axial slices thickness, TE of 160 ms, TR of 9,900 ms, NEX of 1, flip angle of 90°, inversion time of 2,500ms, FOV of 240 x 240 mm, and 256 x 256 matrix in axial plane.

We used the original Digital Imaging and Communications in Medicine (DICOM) format images, and converted to NIfTI format for analysis using MRIcron software. We resliced the images to isovoxels (1.0 x 1.0 x 1.0 mm^3). Then we automatically segmented whole brain structures by recon-all streams of the FreeSurfer development version 7.0 (http://surfer.nmr.mgh.harvard.edu) (Fischl et al., 2002). We segmented the

thalamus automatically from the pre-processed T1 MRI images using the FreeSurfer software. For each subject, we developed the masks of 25 different nuclei, each in both the left and right thalamus, defined by a probabilistic atlas developed with histological data (Iglesias et al., 2018). Among the 25 nuclei, we analyzed the left and right side of the anterior pulvinar (PuA), medial pulvinar (PuM), lateral pulvinar (PuL), and inferior pulvinar (PuI) in the current study.

We measured the volumes of pulvinar subregions and estimated total intracranial volumes (eTIV) using the Freesurfer. We analyzed the four texture features (entropy, contrast, autocorrelation, and cluster shade) of each pulvinar nucleus from T1-weighted MR images using the gray-level co-occurrence matrices (GLCM). The GLCM is an N (number of gray levels) square matrix. Each element (i,j) of the matrix reports how many times specific pairs of gray level values, including a reference voxel i and a neighboring voxel j, occur at distance d and direction θ. Possible combinations of d and θ make the GLCMs, while the matrices are averaged to obtain final GLCM, and the texture features are calculated from the final GLCM (Haralick, Shanmugam, & Dinstein, 1973). For histogram normalization of each pulvinar nucleus, voxels with intensities ranging between $[\mu - 3\sigma, \mu + 3\sigma]$ were included to avoid infrequent intensity values; μ is the mean value of the gray levels and σ is the standard deviation (Collewet, Strzelecki, & Mariette, 2004). Then we quantized gray levels in 8×8 matrices to minimize zero valued entries (Mahmoud-Ghoneim, Alkaabi, de Certaines, & Goettsche, 2008). For the quantization, the 3D GLCMs were generated with a distance of d=1 between voxel pairs and in 13 independent directions (Ortiz, Palacio, Górriz, Ramírez, & Salas-González, 2013). Based on averaged 13 GLCMs, we calculated four texture features in each region. We performed the texture analysis using the MATLAB R2014b (Mathworks, Natick, USA).

2.4. Statistical analysis

We performed descriptive statistics to understand the demographic and clinical data of the two groups. We derived TMT-Diff, which is TMT-B minus TMT-A. We used independent-samples t-test for age and estimated total intracranial volume (eTIV), and chi-square test for sex, clinical dementia rating (CDR), and digit span backward. Educational level, Mini-Mental State Examination (MMSE) scores, digit span forward, and TMT did not follow a normal distribution in normality tests (Kolmogorov-Smirnov or Shapiro-Wilk). Then, we compared these variables with independent-samples Mann-Whitney U test. The digit span test scores were available for 35 NC and 37 DLB, and TMT scores were available for 36 out of 38 DLB patients.

We compared volumes of pulvinar subregions between the DLB group and the NC group to detect whether atrophy progressed in the patient groups. We performed one-way analysis of covariance (ANCOVA), controlling potential confounding effects of age, sex, total years of education, and eTIV. For non-normally distributed data in right PuL, we conducted independent-samples Mann-Whitney U test. In each nucleus, we compared texture feature values among the groups via independent-samples t-test or independent-samples Mann-Whitney U test to evaluate gray level distribution.

We performed a linear regression analysis, entering the texture feature values that were different between the DLB patients and the normal controls as independent variables and the neuropsychological test scores as dependent variables. For the data sets violated normal distribution of residuals, we used log-transformed neuropsychological test scores as dependent variables.

We performed all statistical analyses with the Statistical Package for the Social

Sciences (SPSS) version 20.0 (IBM Corporation, Armonk, NY) on Windows. A p value less than 0.05 was considered statistically significant in the analyses.

3. Results

As summarized in Table 1, DLB patients were comparable to normal controls in age, sex, and educational level. Although DLB patients showed lower MMSE scores than the normal controls, their eTIV were comparable to those of the normal controls. The DLB patients presented lower digit span test scores and longer time to perform the TMT than the normal controls did.

The volumes of the pulvinar and the pulvinar subregions were comparable between DLB patients and the normal controls (Table 2). The texture of the pulvinar was also comparable between the two groups. However, when the texture of the pulvinar subregions were compared separately, DLB patients presented the lower entropy, contrast, and cluster shade than the normal controls, but higher autocorrelation than the normal controls in the left PuM (Table 3). For linear regression analysis with all participants, texture features of left PuM except autocorrelation were positively associated with the performance of MMSE while autocorrelation was negatively associated with MMSE. Entropy and contrast were positively associated with log-transformed digit span forward and digit span backward, and were negatively associated with log TMT (A, B and Diff). In particular, as shown in Figure 2, the texture features had relatively high correlations with log TMT-A (entropy: adjusted $R^2 = 0.231$, $\beta = -0.492$, $p < 0.001$ and contrast: adjusted $R^2 = 0.281$, $\beta = -0.539$, $p < 0.001$) and with log TMT-B (entropy: adjusted $R^2 = 0.226$, $\beta = -0.487$, $p < 0.001$ and contrast: adjusted $R^2 = 0.290$, $\beta = -0.547$, $p < 0.001$). Furthermore, for linear regression analysis with DLB, TMT-Diff was positively associated with autocorrelation (adjusted $R^2 = 0.172$, $\beta = 0.443$, $p = 0.007$) and negatively associated with cluster shade (adjusted $R^2 = 0.105$, $\beta = -0.361$,

p = 0.030) (Figure 3). However, none of the texture features were associated with the performance of MMSE, digit span test, TMT-A and TMT-B ($p > 0.05$).

4. Discussion

The volumes of the pulvinar nuclei were comparable between the DLB patients and the normal controls, which is in line with a previous study by Erskine et al. They reported that the volume of anteromedial pulvinar tissue was not affected by Lewy pathology (Erskine et al., 2017). However, this study found that the texture of left PuM was different between the DLB patients and the normal controls and associated with executive control.

The PuM consists of small, dispersed, and pale neurons (Jones, 2012). We found that DLB patients presented the lower entropy, contrast, and cluster shade than the normal controls, while higher autocorrelation than the normal controls (Table 3). Lower entropy value indicates orderliness of gray level distribution, and smaller contrast value means uniformity of local intensity values among neighboring voxels in an image (Alonso-Caneiro, Szczesna-Iskander, Iskander, Read, & Collins, 2013; Van Griethuysen et al., 2017); meanwhile, lower cluster shade value indicates that the GLCM is skewed to the left in a symmetric image (Alonso-Caneiro et al., 2013; Haralick et al., 1973; Van Griethuysen et al., 2017). Therefore, the DLB patients may have smoother, softer, and more repetitive PuM textures than the normal controls. Previous studies have suggested that the PuM can be affected by Lewy body pathology. According to Erskine et al., alpha-synuclein was most heavily deposited in the PuM among the pulvinar nuclei (Erskine et al., 2017). Furthermore, the PuM interconnects with widespread cerebral cortical regions, such as the frontal cortices, including the orbitofrontal cortex, the dorsolateral prefrontal cortex. The PuM also interconnects with the parieto-temporal association areas, including the superior temporal area, inferior temporal area, and

inferior parietal area, as well as the cingulate and insular cortex (Benarroch, 2015; Romanski et al., 1997; Rosenberg et al., 2008), which are highly affected by Lewy body pathology in DLB (Marui et al., 2002). According to cell-to-cell propagation, alpha synuclein oligomers spread to neurons through anatomically connected networks (Henderson et al., 2019). Alpha synuclein oligomers, which are neurotoxic (Ingelsson, 2016) and exacerbate synaptic degeneration (Rockenstein et al., 2014), may spread to interconnected PuM from neocortical regions and lead to deficient synaptic transmission, as verified in the hippocampus (Diógenes et al., 2012). In contrast to the texture features of pulvinar nuclei, the volume of these may be insensitive to the neuronal changes in the pulvinar nuclei of DLB at an early stage.

We also found that the texture features of left PuM that were different between the DLB patients and the normal controls had higher correlation with the TMT-A and -B scores (Figure 2) than the other neuropsychological test scores. TMT is a neuropsychological test (Rabin, Barr, & Burton, 2005) that is frequently used for screening multiple cognitive processes, such as attention, visual scanning, motoric speed, sequencing, shifting, and flexibility (Strauss, Sherman, & Spreen, 2006). The TMT-A is more likely to associate with attention and the TMT-B is associated with executive function (Arbuthnott & Frank, 2000; Strauss et al., 2006). In linear regression analysis, entropy predicted 24.2% of the variance in log TMT-A scores and 23.7% of the variance in log TMT-B scores having a moderate correlation ($R = 0.492$ and $R = 0.487$), while contrast predicted 29.0% of the variance in log TMT-A scores and 30.0% of the variance in log TMT-B scores presenting a moderate degree of correlation ($R = 0.539$ and $R = 0.547$). However, the texture features explained less than or equal to 15.0% of the variance in MMSE, digit span tests and TMT-Diff having a week correlation ($R < 0.4$). Within DLB, texture features were correlated with TMT-Diff scores (Figure 3). The

TMT-Diff, which is the difference between the TMT-B and TMT-A accounted for set-shifting executive function relatively independent of visual scanning and motor speed (Arbuthnott & Frank, 2000; Corrigan & Hinkeldey, 1987). In the analysis, autocorrelation predicted 19.6% of the variance in TMT-Diff scores presenting a moderate degree of correlation (R = 0.443), while cluster shade predicted 13.1% of the variance in TMT-Diff scores having moderate correlation (R = 0.361). The PuM may involve in executive control that is important feature in early DLB (Collerton, Burn, McKeith, & O'Brien, 2003; McKeith et al., 2005), mirroring the salience network (SN) abnormalities. The SN initiates cognitive control as it modulates the switch between default mode network (DMN) and central executive network (CEN) (Sridharan et al., 2008). For supporting cognitive flexibility, major areas of the SN play an important role: the anterior insula cortex initiates neural switching for accessing attention to salient stimulus and the dorsal anterior cingulate cortex selects the appropriate response (Dajani & Uddin, 2015; Seeley et al., 2007). Damage to the SN has inhibited attention and cognitive control (Li et al., 2019; Menon & Uddin, 2010; Sridharan et al., 2008). The SN can correspond to the PuM because of anatomical interconnections (Benarroch, 2015; Romanski et al., 1997). Also, abnormalities of the PuM have been related to SN connectivity disruption in frontotemporal dementia and in posterior cortical atrophy (Fredericks et al., 2019; S. E. Lee et al., 2014). Consequently, the PuM may represent dysfunction of executive control in DLB.

This study has several limitations. The sample size was small. Intra-scan intensity variation may have affected the estimation of the texture features.

5. Conclusion

This study showed that the texture of left PuM in DLB patients was different from that of normal controls and associated with executive function, which suggests that the left PuM may be impaired and contribute to the development of executive dysfunction in DLB from early stage.

References

Alonso-Caneiro, D., Szczesna-Iskander, D. H., Iskander, D. R., Read, S. A., & Collins, M. J. (2013). Application of texture analysis in tear film surface assessment based on videokeratoscopy. *Journal of Optometry, 6*(4), 185-193.

Arbuthnott, K., & Frank, J. (2000). Trail making test, part B as a measure of executive control: validation using a set-switching paradigm. *Journal of Clinical and Experimental Neuropsychology, 22*(4), 518-528.

Benarroch, E. E. (2015). Pulvinar: associative role in cortical function and clinical correlations. *Neurology, 84*(7), 738-747.

Blanc, F., Colloby, S. J., Cretin, B., de Sousa, P. L., Demuynck, C., O'Brien, J. T., . . . Taylor, J.-P. (2016). Grey matter atrophy in prodromal stage of dementia with Lewy bodies and Alzheimer's disease. *Alzheimer's Research & Therapy, 8*(1), 31.

Blanc, F., Colloby, S. J., Philippi, N., de Pétigny, X., Jung, B., Demuynck, C., . . . Bing, F. (2015). Cortical thickness in dementia with Lewy bodies and Alzheimer's disease: a comparison of prodromal and dementia stages. *PloS One, 10*(6), e0127396.

Bridge, H., Leopold, D. A., & Bourne, J. A. (2016). Adaptive pulvinar circuitry supports visual cognition. *Trends in Cognitive Sciences, 20*(2), 146-157.

Collerton, D., Burn, D., McKeith, I., & O'Brien, J. (2003). Systematic review and meta-analysis show that dementia with Lewy bodies is a visual-perceptual and attentional-executive dementia. *Dementia and Geriatric Cognitive Disorders, 16*(4), 229-237.

Collewet, G., Strzelecki, M., & Mariette, F. (2004). Influence of MRI acquisition protocols and image intensity normalization methods on texture classification. *Magnetic Resonance Imaging, 22*(1), 81-91. doi:10.1016/j.mri.2003.09.001

Corrigan, J. D., & Hinkeldey, N. S. (1987). Relationships between parts A and B of the Trail Making Test. *Journal of Clinical Psychology, 43*(4), 402-409.

Dajani, D. R., & Uddin, L. Q. (2015). Demystifying cognitive flexibility: Implications for clinical and developmental neuroscience. *Trends in Neurosciences, 38*(9), 571-578.

Diógenes, M. J., Dias, R. B., Rombo, D. M., Miranda, H. V., Maiolino, F., Guerreiro, P., . . . Castanho, M. A. (2012). Extracellular alpha-synuclein oligomers modulate synaptic transmission and impair LTP via NMDA-receptor activation. *Journal of Neuroscience, 32*(34), 11750-11762.

Erskine, D., Thomas, A. J., Attems, J., Taylor, J. P., McKeith, I. G., Morris, C. M., & Khundakar, A. A. (2017). Specific patterns of neuronal loss in the pulvinar nucleus in dementia with lewy bodies. *Movement Disorders, 32*(3), 414-422. doi:10.1002/mds.26887

Ferman, T. J., Smith, G. E., Kantarci, K., Boeve, B. F., Pankratz, V. S., Dickson, D. W., . . . Uitti, R. (2013). Nonamnestic mild cognitive impairment progresses to dementia with Lewy bodies. *Neurology, 81*(23), 2032-2038.

Fischl, B., Salat, D. H., Busa, E., Albert, M., Dieterich, M., Haselgrove, C., . . . Klaveness, S. (2002). Whole brain segmentation: automated labeling of neuroanatomical structures in the human brain. *Neuron, 33*(3), 341-355.

Fredericks, C. A., Brown, J. A., Deng, J., Kramer, A., Ossenkoppele, R., Rankin, K., . . . Seeley, W. W. (2019). Intrinsic connectivity networks in posterior cortical atrophy: A role for the pulvinar? *NeuroImage Clin, 21*, 101628.

Goubran, M., Hammond, R. R., de Ribaupierre, S., Burneo, J. G., Mirsattari, S., Steven, D. A., . . . Khan, A. R. (2015). Magnetic resonance imaging and histology correlation in the neocortex in temporal lobe epilepsy. *Annals of Neurology, 77*(2), 237-250.

Gowland, P. A., & Stevenson, V. L. (2003). T1: The Longitudinal Relaxation Time. In P. Tofts (Ed.), *Quantitative MRI of the Brain* (pp. 111-141): John Wiley & Sons.

Han, J. W., Kim, T. H., Kwak, K. P., Kim, K., Kim, B. J., Kim, S. G., . . . Park, J. Y. (2018). Overview of the Korean Longitudinal Study on Cognitive Aging and Dementia. *Psychiatry Investigation, 15*(8), 767.

Haralick, R. M., Shanmugam, K., & Dinstein, I. H. (1973). Textural features for image classification. *IEEE Transactions on Systems, Man, Cybernetics*(6), 610-621.

Henderson, M. X., Cornblath, E. J., Darwich, A., Zhang, B., Brown, H., Gathagan, R. J., . . . Lee, V. M. (2019). Spread of α-synuclein pathology through the brain connectome is modulated by selective vulnerability and predicted by network analysis. *Nature Neuroscience, 22*(8), 1248.

Homman-Ludiye, J., & Bourne, J. A. (2019). The medial pulvinar: function, origin and association with neurodevelopmental disorders. *Journal of Anatomy*.

Iglesias, J. E., Insausti, R., Lerma-Usabiaga, G., Bocchetta, M., Van Leemput, K., Greve, D. N., . . . Paz-Alonso, P. M. (2018). A probabilistic atlas of the human thalamic nuclei combining ex vivo MRI and histology. *Neuroimage, 183*, 314-326. doi:10.1016/j.neuroimage.2018.08.012

Ingelsson, M. (2016). Alpha-synuclein oligomers—neurotoxic molecules in parkinson's disease and other lewy body disorders. *Frontiers in Neuroscience, 10*, 408.

Jones, E. G. (2012). *The thalamus*: Springer Science & Business Media.

Lee, J. H., Lee, K. U., Lee, D. Y., Kim, K. W., Jhoo, J. H., Kim, J. H., . . . Woo, J. I.

(2002). Development of the Korean version of the Consortium to Establish a Registry for Alzheimer's Disease Assessment Packet (CERAD-K): clinical and neuropsychological assessment batteries. *Journals of Gerontology. Series B: Psychological Sciences and Social Sciences, 57*(1), 47-53.

Lee, S. E., Khazenzon, A. M., Trujillo, A. J., Guo, C. C., Yokoyama, J. S., Sha, S. J., . . . Coppola, G. (2014). Altered network connectivity in frontotemporal dementia with C9orf72 hexanucleotide repeat expansion. *Brain, 137*(11), 3047-3060.

Li, L. M., Violante, I. R., Leech, R., Hampshire, A., Opitz, A., McArthur, D., . . . Sharp, D. J. (2019). Cognitive enhancement with Salience Network electrical stimulation is influenced by network structural connectivity. *Neuroimage, 185*, 425-433.

Lowther, E. R., O'Brien, J. T., Firbank, M. J., & Blamire, A. M. (2014). Lewy body compared with Alzheimer dementia is associated with decreased functional connectivity in resting state networks. *Psychiatry Research, 223*(3), 192-201.

Mahmoud-Ghoneim, D., Alkaabi, M. K., de Certaines, J. D., & Goettsche, F.-M. (2008). The impact of image dynamic range on texture classification of brain white matter. *BMC Medical Imaging, 8*(1), 18.

Marui, W., Iseki, E., Nakai, T., Miura, S., Kato, M., Uéda, K., & Kosaka, K. (2002). Progression and staging of Lewy pathology in brains from patients with dementia with Lewy bodies. *Journal of the Neurological Sciences, 195*(2), 153-159.

McKeith, I. G., Dickson, D. W., Lowe, J., Emre, M., O'Brien, J. T., Feldman, H., . . . Consortium on, D. L. B. (2005). Diagnosis and management of dementia with Lewy bodies: third report of the DLB Consortium. *Neurology, 65*(12), 1863-1872. doi:10.1212/01.wnl.0000187889.17253.b1

Menon, V., & Uddin, L. Q. (2010). Saliency, switching, attention and control: a network model of insula function. *Brain Struct Funct., 214*(5-6), 655-667.

Morris, J. C. (1993). The Clinical Dementia Rating (CDR): current version and scoring rules. *Neurology, 43*(11), 2412-2414. doi:10.1212/wnl.43.11.2412-a

Olszewski, J. (1952). *The thalamus of the Macaca Mulatta: An atlas for use with the stereotaxic instrument*: Karger.

Ortiz, A., Palacio, A. A., Górriz, J. M., Ramírez, J., & Salas-González, D. (2013). Segmentation of brain MRI using SOM-FCM-based method and 3D statistical descriptors. *Computational and Mathematical Methods in Medicine, 2013*.

Ouhaz, Z., Fleming, H., & Mitchell, A. S. (2018). Cognitive functions and neurodevelopmental disorders involving the prefrontal cortex and mediodorsal thalamus. *Frontiers in Neuroscience, 12*, 33.

Petrova, M., Pavlova, R., Zhelev, Y., Mehrabian, S., Raycheva, M., & Traykov, L. (2016). Investigation of neuropsychological characteristics of very mild and mild dementia with Lewy bodies. *Journal of Clinical and Experimental Neuropsychology, 38*(3), 354-360.

Rabin, L. A., Barr, W. B., & Burton, L. A. (2005). Assessment practices of clinical neuropsychologists in the United States and Canada: A survey of INS, NAN, and APA Division 40 members. *Archives of Clinical Neuropsychology, 20*(1), 33-65.

Rockenstein, E., Nuber, S., Overk, C. R., Ubhi, K., Mante, M., Patrick, C., . . . Picotti, P. (2014). Accumulation of oligomer-prone α-synuclein exacerbates synaptic and neuronal degeneration in vivo. *Brain, 137*(5), 1496-1513.

Romanski, L., Giguere, M., Bates, J., & Goldman-Rakic, P. (1997). Topographic organization of medial pulvinar connections with the prefrontal cortex in the

rhesus monkey. *Journal of Comparative Neurology, 379*(3), 313-332.

Rongve, A., Soennesyn, H., Skogseth, R., Oesterhus, R., Hortobágyi, T., Ballard, C., . . . Aarsland, D. (2016). Cognitive decline in dementia with Lewy bodies: a 5-year prospective cohort study. *BMJ open, 6*(2), e010357.

Rosenberg, D., Mauguiere, F., Catenoix, H., Faillenot, I., & Magnin, M. (2008). Reciprocal thalamocortical connectivity of the medial pulvinar: a depth stimulation and evoked potential study in human brain. *Cerebral Cortex, 19*(6), 1462-1473.

Seeley, W. W., Menon, V., Schatzberg, A. F., Keller, J., Glover, G. H., Kenna, H., . . . Greicius, M. D. (2007). Dissociable intrinsic connectivity networks for salience processing and executive control. *Journal of Neuroscience, 27*(9), 2349-2356.

Spillantini, M. G., Schmidt, M. L., Lee, V. M.-Y., Trojanowski, J. Q., Jakes, R., & Goedert, M. (1997). α-Synuclein in Lewy bodies. *Nature, 388*(6645), 839.

Sridharan, D., Levitin, D. J., & Menon, V. (2008). A critical role for the right fronto-insular cortex in switching between central-executive and default-mode networks. *Proceedings of the National Academy of Sciences of the United States of America, 105*(34), 12569-12574.

Strauss, E., Sherman, E. M., & Spreen, O. (2006). *A compendium of neuropsychological tests: Administration, norms, and commentary*: Oxford University Press.

Van Griethuysen, J. J., Fedorov, A., Parmar, C., Hosny, A., Aucoin, N., Narayan, V., . . . Aerts, H. J. (2017). Computational radiomics system to decode the radiographic phenotype. *Cancer Research, 77*(21), e104-e107.

Wechsler, D. (1987). *Wechsler memory scale-revised*.

Yoo, S.-W., Kim, Y.-S., Noh, J.-S., Oh, K.-S., Kim, C.-H., NamKoong, K., . . . Min, K.-J. (2006). Validity of Korean version of the mini-international neuropsychiatric

interview. *Anxiety and mood, 2*(1), 50-55.

List of Tables

Table 1. Demographic and clinical characteristics of the participants

	DLB (n = 38)	NC (n = 38)	p*
Age (years, mean±SD)	74.89 ± 6.30	74.84 ± 6.15	0.971
Sex [men, n (%)]	19 (50.00)	19 (50.00)	1.000
Educational level (years, mean±SD)	11.00 ± 5.24	11.45 ± 3.98	0.832
MMSE (points, mean±SD)	19.29 ± 5.43	27.47 ± 1.93	<0.001
Clinical Dementia Rating [n (%)]			<0.001
0	0	38 (100.00)	
0.5	27 (0.71)	0	
1	9 (0.24)	0	
2	2 (0.05)	0	
3	0	0	
Digit span (points, mean±SD)			
Forward	4.38 ± 1.69	7.14 ± 2.57	<0.001
Backward	3.00 ± 1.35	5.20 ± 1.37	<0.001
Trail Making Test (sec, mean±SD)			
A	189.19 ± 116.21	58.26 ± 26.21	<0.001
B	322.94 ± 60.15	181.13 ± 89.52	<0.001
Diff	133.75 ± 98.10	122.87 ± 75.54	0.544
eTIV (mm^3, mean±SD)	1596580.50 ± 167542.68	1565892.06 ± 192721.44	0.461

Abbreviations: DLB = Dementia with Lewy bodies; NC = Normal Controls; MMSE = Mini-Mental State Examination; Trail Making Test-Diff = Trail Making Test-B minus Trail Making Test-A; eTIV = Estimated Total Intracranial Volume

*Student t test, independent-samples Mann-Whitney U test or chi-square test

Table 2. Volumes (mm^3) of pulvinar subregions

Subregion	DLB (n = 38)	NC (n = 38)	p*
Left anterior pulvinar	196.47 ± 28.10	203.15 ± 34.95	0.132
Right anterior pulvinar	164.48 ± 21.59	172.09 ± 23.12	0.054
Left medial pulvinar	917.76 ± 135.68	931.45 ± 137.51	0.304
Right medial pulvinar	760.98 ± 93.68	786.80 ± 110.16	0.121
Left lateral pulvinar	213.14 ± 54.22	198.11 ± 37.21	0.249
Right lateral pulvinar	155.58 ± 22.84	157.22 ± 36.19	0.983
Left inferior pulvinar	192.92 ± 36.11	191.80 ± 28.34	0.741
Right inferior pulvinar	159.84 ± 25.77	155.62 ± 27.84	0.637

Data presented as mean±SD

*One-way analysis of covariance, adjusting confounding factors (age, gender, educational years and eTIV) and independent-samples Mann-Whitney U test for right PuL

Table 3. Texture features for pulvinar nuclei

Texture feature	DLB (n =38)	NC (n = 38)	p*
Left anterior pulvinar			
Entropy	3.17 ± 0.15	3.18 ± 0.17	0.506
Contrast	2.76 ± 0.57	2.81 ± 0.58	0.672
Autocorrelation	18.47 ± 3.00	18.09 ± 3.37	0.611
Cluster shade	-0.94 ± 2.88	-1.37 ± 2.94	0.524
Right anterior pulvinar			
Entropy	3.14 ± 0.14	3.16 ± 0.18	0.528
Contrast	2.93 ± 0.59	2.82 ± 0.63	0.424
Autocorrelation	17.66 ± 2.27	18.69 ± 3.00	0.095
Cluster shade	-0.13 ± 2.25	-0.92 ± 3.00	0.085
Left medial pulvinar			
Entropy	2.93 ± 0.12	3.09 ± 0.16	**< 0.001**
Contrast	1.91 ± 0.25	2.48 ± 0.58	**< 0.001**
Autocorrelation	18.91 ± 1.74	17.38 ± 2.85	**0.006**
Cluster shade	-2.13 ± 1.95	0.16 ± 3.45	**< 0.001**
Right medial pulvinar			
Entropy	2.96 ± 0.09	2.97 ± 0.11	0.662
Contrast	1.92 ± 0.20	1.92 ± 0.23	0.979
Autocorrelation	19.63 ± 2.17	19.38 ± 2.04	0.648
Cluster shade	-1.88 ± 2.03	-1.78 ± 2.20	0.828
Left lateral pulvinar			
Entropy	3.11. ± 0.15	3.10. ± 0.16	0.679
Contrast	2.57 ± 0.43	2.51 ± 0.56	0.588
Autocorrelation	16.33 ± 2.75	17.26 ± 2.91	0.155
Cluster shade	0.86 ± 2.58	0.35 ± 3.52	0.470
Right lateral pulvinar			
Entropy	3.06 ± 0.19	3.06 ± 0.21	0.947
Contrast	2.67 ± 0.49	2.57 ± 0.60	0.437
Autocorrelation	17.42 ± 3.00	17.68 ± 2.80	0.694
Cluster shade	1.51 ± 2.88	1.32 ± 3.31	0.789
Left inferior pulvinar			
Entropy	3.01 ± 0.19	3.04 ± 0.18	0.390
Contrast	2.50 ± 0.59	2.51 ± 0.57	0.947
Autocorrelation	19.33 ± 2.49	18.42 ± 2.40	0.112
Cluster shade	-0.31 ± 1.64	-0.28 ± 1.74	0.949
Right inferior pulvinar			
Entropy	2.88 ± 0.24	2.90 ± 0.27	0.726
Contrast	2.29 ± 0.57	2.30 ± 0.59	0.928
Autocorrelation	18.61 ± 3.12	19.05 ± 3.10	0.542
Cluster shade	0.19 ± 2.52	-0.16 ± 2.38	0.542

Values are mean±SD

* Student t test or independent-samples Mann-Whitney U test

List of Figures

Figure 1. Masks of pulvinar nuclei overlaying on normalized T1-weighted magnetic resonance image

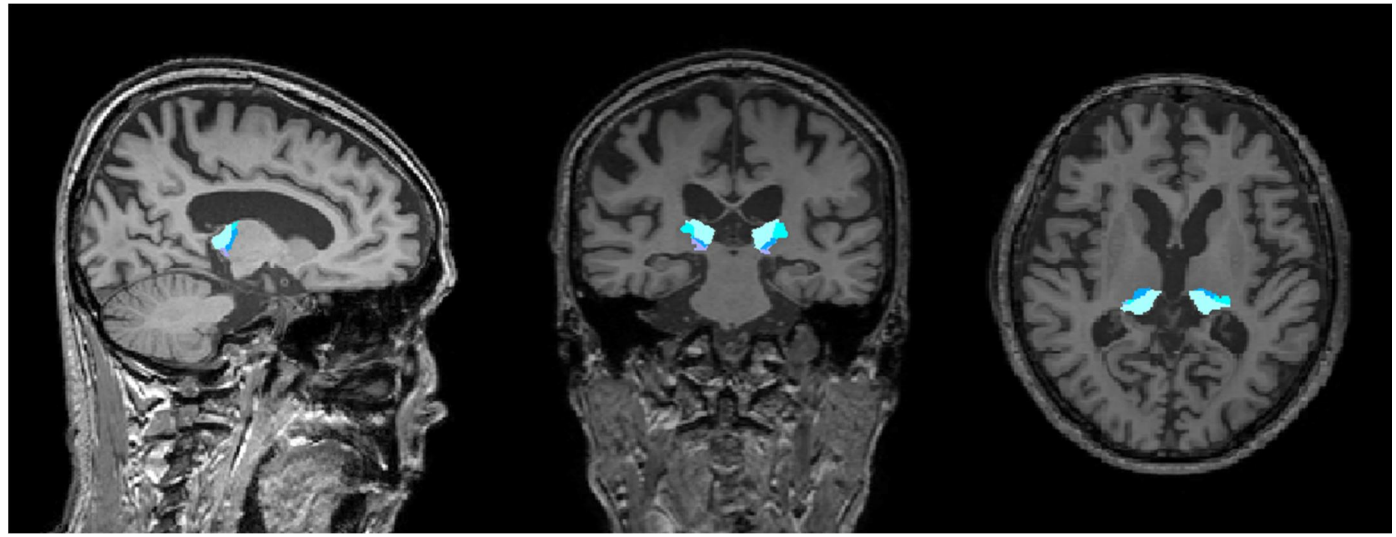

Figure 2. Association between log-transformed TMT scores and texture features for all participants

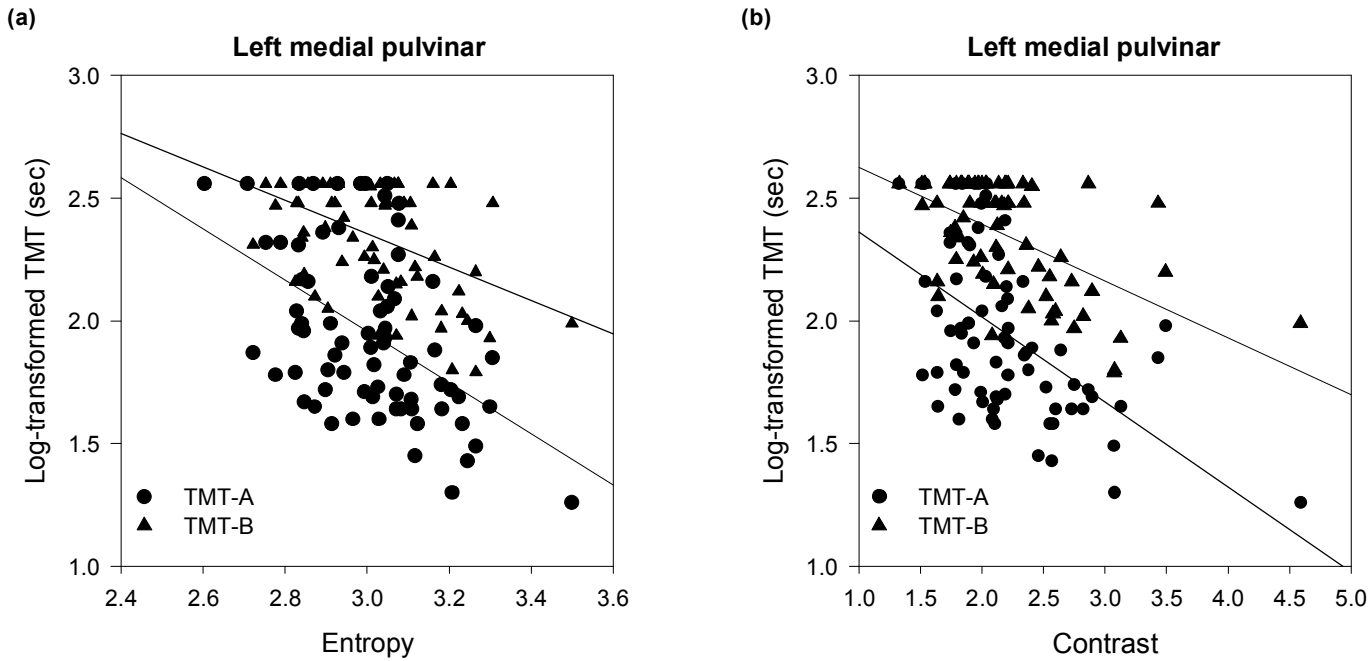

(a) TMT-A: adjusted $R^2 = 0.231$, $\beta = -0.492$, $p < 0.001$; TMT-B: adjusted $R^2 = 0.226$, $\beta = -0.487$, $p < 0.001$ (b) TMT-A: adjusted $R^2 = 0.281$, $\beta = -0.539$, $p < 0.001$; TMT-B: adjusted $R^2 = 0.290$, $\beta = -0.547$, $p < 0.001$

*Linear regression analysis

Figure 3. Association between derived TMT scores and texture features for DLB

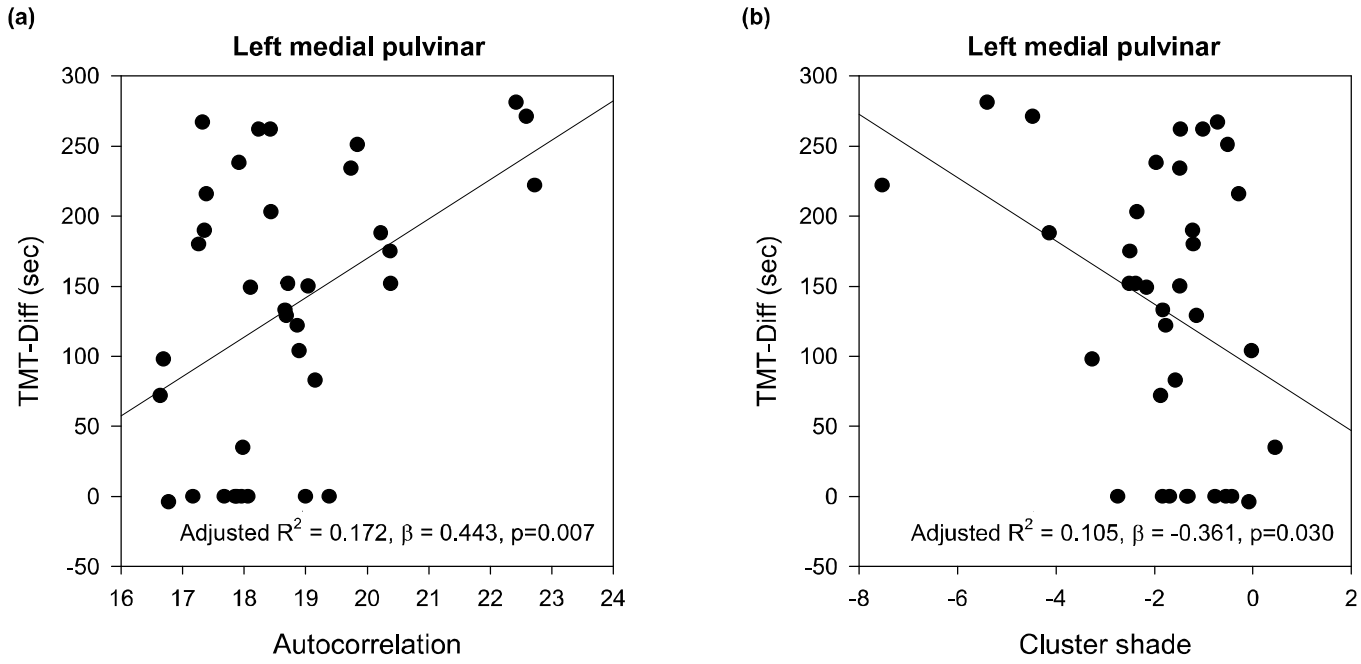

TMT-Diff = Trail Making Test-B minus Trail Making Test-A

*Linear regression analysis

국문 초록

루이소체 치매 환자에서 내측 베개핵의 자기 공명 영상 텍스처 변화

탁 가 영

서울대학교 대학원

뇌인지과학과 뇌인지과학전공

배경: 루이소체 치매에서 집행기능의 장애는 일반적이다. 베개핵은 집행기능에 기여한다고 알려져 있으며 루이소체 병리에 취약한 현출성 네트워크의 대뇌 피질 영역과 동기화된다는 보고가 있었다.

목적: 본 연구는 경도 루이소체 치매 환자들에서 베개핵의 구조적 변화를 확인하고 이러한 변화와 집행기능과의 연관성을 연구하였다.

방법: 연구의 대상자는 38명의 루이소체 치매 환자들과 38명의 연령과 나이가 매칭되는 정상 대조군으로 구성하였다. 참여한 피험자들의 인지기능은 the Consortium to Establish a Registry for Alzheimer's Disease Assessment Packet (CERAD-K)로 평가하였다. 전처리한 T1

가중 자기 공명 영상을 사용하여 4개의 베개핵을 추출하였다. 각 핵에 대한 부피와 텍스처 피처 값을 루이소체 치매 환자와 정상 대조군사이에서 비교하였다. 또한 텍스처와 신경심리검사 점수의 연관성을 확인하기 위하여 선형회귀를 사용하였다.

결과: 루이소체 치매 환자들은 모든 베개핵에서 정상 대조군과 유사한 부피를 나타냈다. 하지만 왼쪽 내측 베개핵에서 텍스처의 차이를 보였다. 루이소체 치매환자들은 정상 대조군에 비해 왼쪽 내측 베개핵의 entropy, contrast와 cluster shade는 더 낮고 autocorrelation은 더 높았다. 이러한 텍스처의 특징들은 trail making tests로 측정된 전환 능력과 관련이 있었다.

결론: 루이소체 치매 환자에서 왼쪽 내측 베개핵은 초기 단계부터 구조적으로 변화할 수 있고, 이는 집행 기능 장애의 발전에 기여할 수 있다.

주요어: 루이소체 치매, 베개핵, 텍스처 분석, 명암도 동시발생 행렬(GLCM)

학 번 : 2017-25754